

Electronic Supporting Information

**Harnessing the Dual Role of DMSO in the Synthesis of
SbOCl·DMSO: An Excellent UV Nonlinear Optical Crystal with
Unique 1D Spiral Chain**

Xiande Peng,^a Xiangyuan Li,^a Yingzi Zhang,^a Xuehua Dong,^{*a} Ling Huang,^a Liling Cao,^a Daojiang Gao^a and Guohong Zou^{*b}

^a College of Chemistry and Materials Science, Sichuan Normal University, Chengdu, 610066, P. R. China.

^b College of Chemistry, Sichuan University, Chengdu, 610065, P. R. China.

E-mail: dongxh027@sina.com; zough@scu.edu.cn

Table of contents

| Sections | Titles | Pages |
|------------|--|---------|
| Section S1 | Experimental section (Instrumentations and Computational Descriptions). | S3-S4 |
| Table S1 | Crystal data and structure refinement for SbOCl·DMSO. | S5 |
| Table S2 | Atomic coordinates and equivalent isotropic displacement parameters for SbOCl·DMSO. $U_{(eq)}$ is defined as one third of the trace of the orthogonalized U_{ij} tensor. | S6 |
| Table S3 | Selected Bond lengths [Å] and angles [°] for SbOCl·DMSO. | S7 |
| Table S4 | Calculation of dipole moments for $[SbO_3Cl]^{4-}$ for a unit cell in SbOCl·DMSO (D = Debyes). | S8 |
| Table S5 | The summary of optical properties of most Sb-based oxygen-containing acid salt NLO crystals. | S9 |
| Figure S1 | (a) TGA curve of SbOCl·DMSO (b) Powder XRD pattern of the residue of TGA for SbOCl·DMSO. | S10 |
| Figure S2 | IR spectrum of compound SbOCl·DMSO. | S10 |
| Figure S3 | The calculated band gap of compound SbOCl·DMSO. | S11 |
| References | | S12-S15 |

Section S1. Experimental section

Instrumentations.

Suitable single crystals were selected under an optical microscope. Crystal structures determination of SbOCl·DMSO was performed on a Bruker SMART BREEZE diffractometer with graphite-monochromated MoK α radiation ($\lambda = 0.71073 \text{ \AA}$) at room temperature. All absorption corrections were performed by using the SADABS program. The structure was solved by direct methods and refined by full-matrix least squares on F² using the SHELX-97 program package.^{1,2} All of the structures were verified using the ADDSYM algorithm from the program PLATON and no higher symmetries were found.³ Crystallographic data and structural refinements for the compound are summarized in Table S1. Atomic coordinates and isotropic displacement coefficients, and selected bond lengths for the compound are listed in Tables S2-S4.

Powder XRD pattern was obtained using a Rigaku Smartlab powder X-ray diffractometer with CuK α radiation ($\lambda = 1.54056 \text{ \AA}$), in the angular range of $2\theta = 5\text{-}50^\circ$, and with a scan step width of 0.05° and a fixed time of 0.2 s.

Thermogravimetric analysis (TGA) was performed on a Netzsch STA 409 PC. A 10 mg crystal sample was sealed in a platinum crucible and heated from room temperature to 720°C at a rate of 10 °C/min in a N₂ atmosphere.

An infrared spectrum in the range of 4000-400 cm⁻¹ was recorded on a Vertex 70 Fourier transform infrared (FT-IR) spectrometer with KBr as the diluent. KBr (100 mg) and solid sample (1 mg) were fully ground in an agate mortar, and a special tabletting device was used to press the sample into a transparent sheet with a diameter of 13 mm and a thickness of about 1 mm for analysis.

The UV-vis diffuse reflectance spectrum of SbOCl·DMSO was recorded using a Shimadzu UV-2600 spectrophotometer with BaSO₄ plate as a standard (100% reflectance). The Kubelka-Munk function is used to calculate the absorption spectrum from the reflection spectrum: $F(R) = \alpha/S = (1-R)^2/2R$, where R is the reflectance, α is the absorption coefficient, and S is the scattering coefficient.⁴

The birefringence of SbOCl·DMSO was characterized by using the polarizing microscope equipped (ZEISS Axio Scope. A1) with Berek compensator. The wavelength of the light source

was 546 nm. Owing to the clear boundary lines of the first-, second- and third-order interference color, the relative error was small enough. Before the scanning, the small and transparent SbOCl·DMSO crystal was chosen to measure, in order to improve the accuracy of the birefringence. The formula for calculating the birefringence is listed below,

$$R = |N_e - N_o| \times T = \Delta n \times T$$

Here, R represents the optical path difference, Δn means the birefringence, and T denotes the thickness of the crystal.

Computational Descriptions.

The first-principles calculation of SbOCl·DMSO was carried out by using the CASTEP software package to understand the relationship between structure and properties.⁵ The band structure, density of states (DOS)/partial DOS (PDOS), birefringence and electron-density difference map of SbOCl·DMSO was computed. The generalized gradient approximation (GGA) with Perdew-Burke-Emzerh (PBE) functional was adopted for all calculations.⁶ Norm-conserving were employed for all the atoms.⁷ The criteria of convergences of energy are set as 1.0e-6 eV/atom. The kinetic energy cutoff of 800 eV and the k-point sampling of $2 \times 6 \times 2$ were chosen for SbOCl·DMSO.⁸ The rest parameters used in the calculations were set by the default values of the CASTEP. The valences of composed atoms were as follow: O, 2s²p⁶; Cl, 3s²3p⁵; Sb, 5s²5p³; C, 2S²2P²; S, 3S²3P⁴.

To obtain the linear optical properties, the complex dielectric function $\varepsilon(\omega) = \varepsilon_1(\omega) + i\varepsilon_2(\omega)$ has been determined in the random phase approximation from the PBE wavefunctions. The imaginary part of the dielectric function due to direct inter-band transitions is given by the expression,

$$\varepsilon_2(\hbar\omega) = \frac{2e^2\pi}{\Omega\varepsilon_0} \sum_{k,v,c} \left| \langle \psi_k^c | u \cdot r | \psi_k^v \rangle \right|^2 \delta(E_k^c - E_k^v - E)$$

where Ω , ω , u , v and c are the unit-cell volume, photon frequencies, the vector defining the polarization of the incident electric field, valence and conduction bands, respectively. The real part of the dielectric function is obtained from ε_2 by a Kramers-Kronig transformation,

$$\varepsilon_1(\omega) = 1 + \left(\frac{2}{\pi} \right) \int_0^{+\infty} d\omega' \frac{\omega'^2 \varepsilon_2(\omega)}{\omega'^2 - \omega^2}$$

Table S1. Crystal data and structure refinement for SbOCl·DMSO.

| Compound | SbOCl·DMSO |
|---|--------------------------|
| Formula Mass | 251.33 |
| Crystal System | orthorhombic |
| Space Group | <i>Pca2</i> ₁ |
| <i>a</i> (Å) | 16.2952 (6) |
| <i>b</i> (Å) | 5.8104 (2) |
| <i>c</i> (Å) | 14.2328 (5) |
| α (°) | 90 |
| β (°) | 90 |
| γ (°) | 90 |
| <i>V</i> (Å ³) | 1347.58 (8) |
| <i>Z</i> | 8 |
| ρ (calcd) (g/cm ³) | 2.478 |
| Temperature (K) | 303.38 (10) |
| λ (Å) | 0.71073 |
| <i>F</i> (000) | 944.0 |
| μ (mm ⁻¹) | 4.703 |
| <i>R</i> ₁ , <i>wR</i> ₂ (<i>I</i> >2σ(<i>I</i>)) ^a | 0.0286 / 0.0620 |
| GOF on <i>F</i> ² | 1.002 |

^a $R_1(F) = \sum ||F_o| - |F_c|| / \sum |F_o|$. $wR_2(F_o^2) = [\sum w(F_o^2 - F_c^2)^2 / \sum w(F_o^2)^2]^{1/2}$

Table S2. Atomic coordinates and equivalent isotropic displacement parameters for SbOCl·DMSO. U_{eq} is defined as one third of the trace of the orthogonalized U_{ij} tensor.

| atom | <i>x</i> | <i>y</i> | <i>z</i> | $U_{\text{eq}}(\text{\AA}^2)$ |
|------|--------------|--------------|--------------|-------------------------------|
| Sb1 | 0.34421 (2) | 0.58020 (6) | 0.53725 (3) | 0.02660 (11) |
| Sb2 | 0.44502 (3) | 1.07994 (6) | 0.59428 (2) | 0.02724 (11) |
| S1 | 0.39303 (11) | 0.50190 (3) | 0.31654 (12) | 0.0361 (3) |
| S2 | 0.57890 (12) | 0.94450 (3) | 0.42594 (13) | 0.0382 (4) |
| Cl1 | 0.28613 (12) | 1.08920 (3) | 0.63138 (13) | 0.0402 (4) |
| Cl2 | 0.41277 (14) | 0.58160 (3) | 0.70600 (12) | 0.0431 (4) |
| O1 | 0.42440 (3) | 0.33750 (7) | 0.50870 (3) | 0.0278 (9) |
| O2 | 0.41760 (3) | 0.83550 (7) | 0.50440 (3) | 0.0287 (9) |
| O3 | 0.32040 (3) | 0.55210 (8) | 0.38370 (3) | 0.0385 (11) |
| O4 | 0.56780 (3) | 1.05660 (8) | 0.52310 (4) | 0.0429 (12) |
| C1 | 0.38890 (5) | 0.20170 (12) | 0.29580 (5) | 0.0449 (17) |
| C2 | 0.60240 (5) | 0.65180 (13) | 0.44910 (6) | 0.0518 (19) |
| C3 | 0.67860 (6) | 1.03730 (16) | 0.39070 (6) | 0.057 (2) |
| C4 | 0.35360 (6) | 0.59790 (13) | 0.20600 (6) | 0.055 (2) |

Table S3. Selected Bond lengths [Å] and angles [°] for SbOCl·DMSO.

| | | | |
|--------------------------|-------------|---------------------------|-------------|
| Sb1—Cl2 | 2.6492 (18) | Sb2—O4 | 2.246 (5) |
| Sb1—O1 | 1.965 (4) | S1—O3 | 1.550 (6) |
| Sb1—O2 | 1.961 (4) | S1—C1 | 1.770 (7) |
| Sb1—O3 | 2.225 (5) | S1—C4 | 1.789 (9) |
| Sb2—Cl1 | 2.6430 (19) | S2—O4 | 1.539 (5) |
| Sb2—O1 ⁱ | 1.959 (4) | S2—C2 | 1.774 (8) |
| Sb2—O2 | 1.963 (4) | S2—C3 | 1.784 (9) |
| O1—Sb1—Cl2 | 85.20 (13) | O4—Sb2—Cl1 | 164.50 (14) |
| O1—Sb1—O3 | 81.98 (17) | O3—S1—C2 | 105.0 (3) |
| O2—Sb1—Cl2 | 87.09 (13) | O3—S1—C4 | 102.1 (4) |
| O2—Sb1—O1 | 95.06 (18) | C1—S1—C4 | 98.5 (4) |
| O2—Sb1—O3 | 85.87 (18) | O4—S2—C2 | 105.3 (3) |
| O3—Sb1—Cl2 | 164.76 (15) | O4—S2—C3 | 103.4 (4) |
| O1 ⁱ —Sb2—Cl1 | 86.60 (13) | C2—S2—C3 | 98.4 (4) |
| O1 ⁱ —Sb2—O2 | 96.24 (18) | Sb2 ⁱⁱ —O1—Sb1 | 122.28 (19) |
| O1 ⁱ —Sb2—O4 | 85.32 (18) | Sb1—O2—Sb2 | 122.1 (2) |
| O2—Sb2—Cl1 | 85.50 (13) | S1—O3—Sb1 | 119.1 (3) |
| O2—Sb2—O4 | 82.26 (17) | S2—O4—Sb2 | 112.4 (3) |

Symmetry codes: (i) $x, 1+y, z$; (ii) $x, -1+y, z$.

Table S4. Calculation of dipole moments for $[\text{SbO}_3\text{Cl}]^4-$ for a unit cell in $\text{SbOCl}\cdot\text{DMSO}$ ($D = \text{Debyes}$)

| SbOCl·DMSO | | | | |
|--------------------------------|----------------------------|---------------------|---------------------|-----------------|
| Polar unit (aunit cell) | Dipole moment (D) | | | |
| | <i>x</i> -component | <i>y</i> -component | <i>z</i> -component | total magnitude |
| $[\text{SbO}_3\text{Cl}]^{4-}$ | -10.61955962 | -0.379347141 | 16.89283923 | 19.95712825 |
| | 19.77404905 | -0.076006172 | 1.729476859 | 19.84968219 |
| | -10.62272863 | 0.376417749 | 16.88926103 | 19.95573081 |
| | 19.77404905 | 0.076006172 | 1.729476859 | 19.84968219 |
| | 10.62269352 | -0.376414555 | 16.88925601 | 19.95570781 |
| | -19.77401349 | -0.07600263 | 1.729535724 | 19.84965188 |
| | 10.62269352 | 0.376414555 | 16.88925601 | 19.95570781 |
| | -19.77401349 | 0.07600263 | 1.729535724 | 19.84965188 |
| | U_x | U_y | U_z | U_t |
| total | 0.000396238 | -0.002929392 | 74.47864 | 74.47864 |
| Cell Volume | $1347.58(8) \text{ \AA}^3$ | | | |

Table S5. The summary of optical properties of most Sb-based oxygen-containing acid salt NLO crystals.

| number | Crystal | Dimension | SHG (×KDP) | Birefringent | Ref. |
|--------|---|-----------|---------------|---------------|-----------|
| 1 | (C ₅ H ₅ NO)(Sb ₂ OF ₄) | 0D | 12 | 0.513@546 nm | 9 |
| 2 | Rb ₂ SbFP ₂ O ₇ | 2D | 5.1 | 0.15@546 nm | 10 |
| 3 | BaSb(H ₂ PO ₂) ₃ Cl ₂ | 2D | 5 | 0.09@546 nm | 11 |
| 4 | SbOCl·DMSO | 1D | 4.4 | 0.084@546 nm | this work |
| 5 | K ₂ Sb(P ₂ O ₇)F | 2D | 4 | 0.157@546 nm | 12 |
| 6 | SbF ₃ ·glycine | 0D | 3.6 | 0.057@1064 nm | 13 |
| 7 | SbB ₃ O ₆ | 2D | 3.5 | 0.29@546 nm | 14 |
| 8 | (NH ₄) ₃ SbF ₃ (NO ₃) ₃ | 0D | 3.3 | 0.098@546 nm | 15 |
| 9 | CsSbF ₂ SO ₄ | 1D | 3 | 0.112@1064nm | 16 |
| 10 | Rb ₂ SbF ₃ (NO ₃) ₂ | 2D | 2.7 | 0.06@1064 nm | 17 |
| 11 | RbSbSO ₄ Cl ₂ | 1D | 2.7 | 0.11@1064 nm | 18 |
| 12 | Rb ₃ SbF ₃ (NO ₃) ₃ | 0D | 2.2 | 0.1@546 nm | 19 |
| 13 | (SbTeO ₃)(NO ₃) | 2D | 2.2 | 0.081@546 nm | 20 |
| 14 | Rb ₂ Sb(C ₂ O ₄)Cl ₃ | 0D | 2.1 | 0.22@546nm | 21 |
| 15 | Sb ₆ O ₇ (SO ₄) ₂ | 3D | 2 | 0.052@1064 nm | 22 |
| 16 | (NH ₄) ₂ Sb(C ₂ O ₄)Cl ₃ | 0D | 1.8 | 0.27@546nm | 21 |
| 17 | (NH ₄)SbCl ₂ (SO ₄) | 1D | 1.7 | 0.09@1064 nm | 23 |
| 18 | K ₂ Sb(C ₂ O ₄)Cl ₃ | 0D | 1.6 | 0.21@546nm | 21 |
| 19 | (C ₅ H ₆ N)SbF ₂ SO ₄ | 1D | 1.6 | 0.179@546nm | 24 |
| 20 | RbSb ₂ (C ₂ O ₄)F ₅ | 0D | 1.3 | 0.09@546 nm | 25 |
| 21 | Sb ₄ O ₄ (SO ₄)(OH) ₂ | 3D | 1.2 | 0.147@1064nm | 26 |
| 22 | NH ₄ Sb ₂ (C ₂ O ₄)F ₅ | 0D | 1.1 | 0.111@546 nm | 27 |
| 23 | RbSbF ₂ SO ₄ | 1D | 0.96 | 0.1@1064 nm | 28 |
| 24 | NH ₄ SbF ₂ SO ₄ | 1D | 0.7 | 0.138@1064 nm | 29 |
| 25 | Rb ₂ SO ₄ ·(SbF ₃) ₂ | 1D | 0.5 | 0.11@1064 nm | 30 |
| 26 | CsSb(SO ₄) ₂ | 1D | 0.35 | 0.174@546nm | 31 |
| 27 | β-NaSb ₃ P ₂ O ₁₀ | 2D | 0.35 | 0.072@1064 nm | 32 |
| 28 | Rb ₂ SO ₄ ·SbF ₃ | 1D | 0.3 | 0.09@1064 nm | 33 |
| 29 | NH ₄ Sb(SO ₄) ₂ | 1D | 0.2 | 0.15@546 nm | 34 |
| 30 | K ₂ Sb ₂ (C ₂ O ₄)F ₆ | 1D | 0.1 | 0.097@546 nm | 35 |
| 31 | K ₂ SO ₄ ·SbF ₃ | 1D | 0.1 | 0.08@1064 nm | 33 |
| 32 | K ₄ Sb(SO ₄) ₃ Cl | 0D | 0.1 | 0.066@546 nm | 36 |
| 33 | Rb ₆ Sb ₄ (SO ₄) ₃ F ₁₂ | 0D | 0.1 | 0.01@1046 nm | 37 |

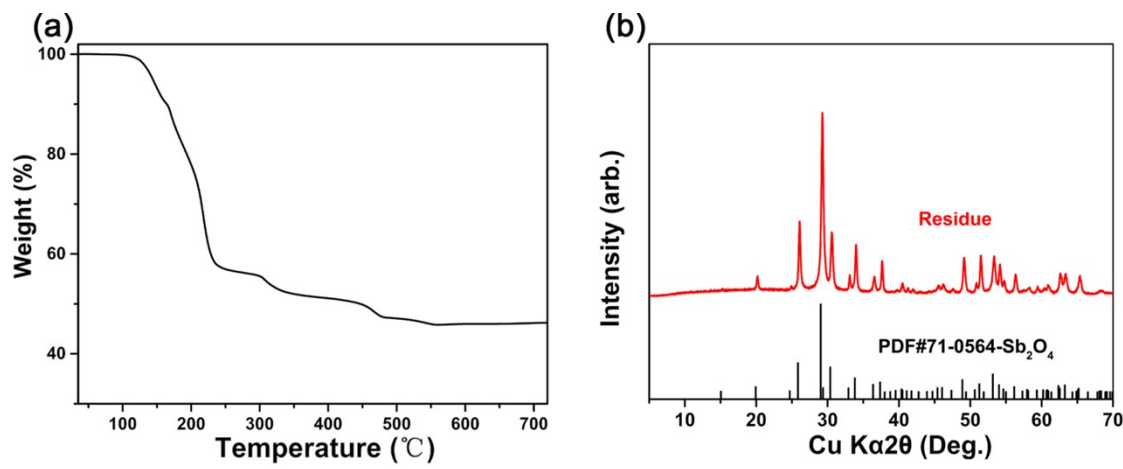


Figure S1. (a) TGA curve of SbOCl·DMSO (b) Powder XRD patterns of the residue of TGA for SbOCl·DMSO.

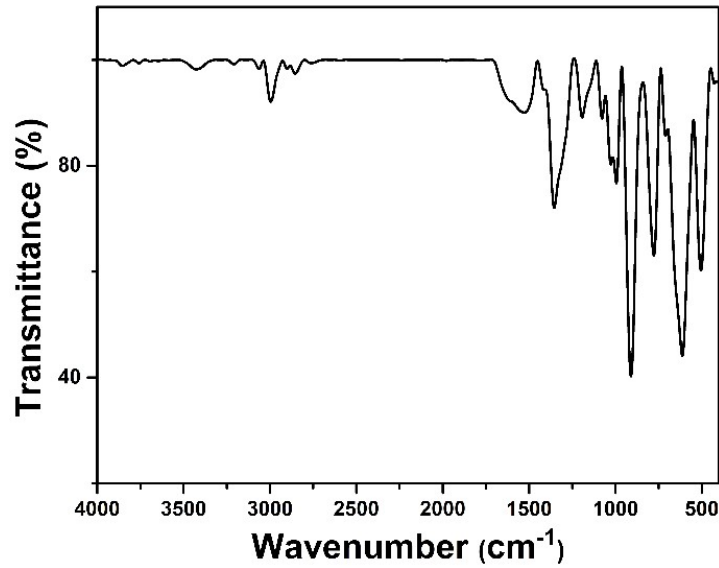


Figure S2. IR spectrum of compound SbOCl·DMSO.

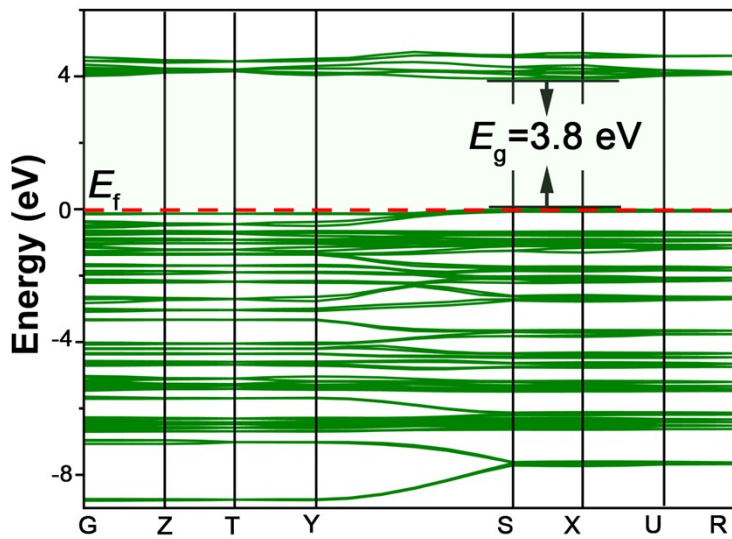


Figure S3. The calculated band gap of compound SbOCl·DMSO.

References

- [1] Sheldrick, G. M. A Short History of SHELX, *Acta Crystallogr A*. 2008, **64**, 112-122.
- [2] Sheldrick, G. M. SHELXTL-97, Program for Crystal Structure Solution. University of Göttingen, Germany, 1997.
- [3] A. Spek, Single-crystal structure validation with the program PLATON, *J. Appl. Cryst.* 2003, **36**, 7-13.
- [4] (a) Kubelka, P.; Munk, F. An Article on Optics of Paint Layers. *Z. Technol. Phys.* 1931, **12**, 593-601; (b) Tauc, J. Absorption edge and internal electric fields in amorphous semiconductors. *Mater. Res. Bull.* 1970, **5**, 721-729.
- [5] Clark, S. J.; Segall, M. D.; Pickard, C. J.; Hasnip, P. J.; Probert, M. J.; Refson, K.; Payne, M. C. First principles methods using CASTEP. *Z. Kristall.* 2005, **220**, 567-570.
- [6] Vanderbilt, D. Soft self-consistent pseudopotentials in a generalized eigenvalue formalism. *Phys. Rev. B*. 1990, **41**, 7892-7895.
- [7] Kobayashi, K. Norm-conserving Pseudopotential Database (NCPS97). *Computational Materials Science*. 1999, **14**, 72-76.
- [8] Monkhorst, H. J.; Pack, J. D. Special Points for Brillouin-Zone Integrations. *Phys. Rev. B*. 1976, **13**, 5188-5192.
- [9] L. Qi, X. X. Jiang, K. N. Duanmu, C. Wu, Z. S. Lin, Z. P. Huang, M. G. Humphrey and C. Zhang, Record Second-Harmonic Generation and Birefringence in an Ultraviolet Antimonate by Bond Engineering, *J. Am. Chem. Soc.*, 2024, **146**, 9975–9983.
- [10] X. H. Dong, H. B. Huang, L. Huang, Y. Q. Zhou, B. B. Zhang, H. M. Zeng, Z. E. Lin and G. H. Zou, Unearthing Superior Inorganic UV Second-Order Nonlinear Optical Materials: A Mineral-Inspired Method Integrating First-Principles High-Throughput Screening and Crystal Engineering, *Angew. Chem. Int. Ed.*, 2024, **63**, e202318976.
- [11] Y. Long, X. H. Dong, L. Huang, H. M. Zeng, Z. E. Lin, L. Zhou and G. H. Zou, BaSb(H₂PO₂)₃Cl₂: An Excellent UV Nonlinear Optical Hypophosphate Exhibiting Strong Second-harmonic Generation Response, *Mater. Today Phys.*, 2022, **28**, 100876.
- [12] S. V. Krivovichev and L. Bindi, Correspondence on “K₂Sb(P₂O₇)F: Cairo Pentagonal Layer with Bifunctional Genes Reveal Optical Performance” *Angew. Chem. Int. Ed.*, 2021, **60**, 3854–

3855.

- [13] Z. Y. Bai, J. Lee, C. L. Hu, G. H. Zou and K. M. Ok, Hydrogen Bonding Bolstered Head-to-Tail Ligation of Functional Chromophores in a 0D SbF₃·glycine Adduct for a Short-Wave Ultraviolet Nonlinear Optical Material, *Chem. Sci.*, 2024, **15**, 6572–6576.
- [14] Y. C. Liu, X. M. Liu, S. Liu, Q. R. Ding, Y. Q. Li, L. N. Li, S. G. Zhao, Z. S. Lin, J. H. Luo and M. C. Hong, An Unprecedented Antimony(III) Borate with Strong Linear and Nonlinear Optical Responses *Angew. Chem. Int. Ed.*, 2020, **132**, 7867–7870.
- [15] Q. Wang, J. X Ren, D. Wang, L. L. Cao, X. H. Dong, L. Huang, D. J. Gao and G. H. Zou, Low Temperature Molten Salt Synthesis of Noncentrosymmetric (NH₄)₃SbF₃(NO₃)₃ and Centrosymmetric (NH₄)₃SbF₄(NO₃)₂, *Inorg. Chem. Front.*, 2023, **10**, 2107–2114.
- [16] X. H. Dong, L. Huang, C. F. Hu, H. M. Zeng, Z. E. Lin, X. Wang, K. M. Ok and G. H. Zou, CsSbF₂SO₄: An Excellent Ultraviolet Nonlinear Optical Sulfate with a KTiOPO₄ (KTP)-type Structure *Angew. Chem. Int. Ed.*, 2019, **58**, 6528–6534.
- [17] L. Wang, H. M. Wang, D. Zhang, D. J. Gao, J. Bi, L. Huang and G. H. Zou, Centrosymmetric RbSnF₂NO₃ vs. Noncentrosymmetric Rb₂SbF₃(NO₃)₂, *Inorg. Chem. Front.*, 2021, **8**, 3317–3324.
- [18] F. F. He, Y. L. Deng, X. Y. Zhao, L. Huang, D. J. Gao, J. Bi, X. Wang and G. H. Zou, RbSbSO₄Cl₂: an Excellent Sulfate Nonlinear Optical Material Generated Due to the Synergistic Effect of Three Asymmetric Chromophores, *J. Mater. Chem. C*, 2019, **7**, 5748–5754.
- [19] L. Wang, F. Yang, X. Y. Zhao, L. Huang, D. J. Gao, J. Bi, X. Wang and G. H. Zou, Rb₃SbF₃(NO₃)₃: an Excellent Antimony Nitrate Nonlinear Optical Material with a Strong Second Harmonic Generation Response Fabricated by a Rational Multi-component Design, *Dalton Trans.*, 2019, **48**, 15144–15150.
- [20] B. Zhang, C. L. Hu, J. G. Mao and F. Kong, Fully Tricoordinated Assembly Unveils a Pioneering Nonlinear Optical Crystal (SbTeO₃)(NO₃), *Chem. Sci.*, 2024, **15**, 18549–18556.
- [21] D. Zhang, Q. Wang, H. Luo, L. L. Cao, X. H. Dong, L. Huang, D. J. Gao and G. H. Zou, Deep Eutectic Solvents Synthesis of A₂Sb(C₂O₄)Cl₃ (A = NH₄, K, Rb) with Superior Optical Performance, *Adv. Opt. Mater.*, 2023, **11**, 2202874.
- [22] Q. Wei, C. He, K. Wang, X. F. Duan, X. T. An, J. H. Li and G. M. Wang, Sb₆O₇(SO₄)₂: A Promising Ultraviolet Nonlinear Optical Material with an Enhanced Second-harmonic-generation Response Activated by Sb^{III} Lone-Pair Stereoactivity, *Chem. Eur. J.*, 2021, **27**, 5880–5884.

- [23] F. F. He, Q. Wang, C. F. Hu, W. He, X. Y. Luo, L. Huang, D. J. Gao, J. Bi, X. Wang and G. H. Zou, Centrosymmetric $(\text{NH}_4)_2\text{SbCl}(\text{SO}_4)_2$ and Non-centrosymmetric $(\text{NH}_4)\text{SbCl}_2(\text{SO}_4)$: Synergistic Effect of Hydrogen-Bonding Interactions and Lone-Pair Cations on the Framework Structures and Macroscopic Centricities, *Crystal Growth & Design*, 2018, **18**, 6239–6247.
- [24] P. Zhang, X. Mao, X. H. Dong, L. Huang, L. L. Cao, D. J. Gao and G. H. Zou, Two UV Organic-inorganic Hybrid Antimony-based Materials with Superior Optical Performance Derived from Cation-anion Synergetic Interactions, *Chin. Chem. Lett.*, 2024, **35**, 109235.
- [25] W. Y. Wang, X. Y. Wang, L. Xu, D. Zhang, J. L. Xue, S. Y. Wang, X. H. Dong, L. L. Cao, L. Huang and G. H. Zou, Centrosymmetric $\text{Rb}_2\text{Sb}(\text{C}_2\text{O}_4)_{2.5}(\text{H}_2\text{O})_3$ and Noncentrosymmetric $\text{RbSb}_2(\text{C}_2\text{O}_4)\text{F}_5$: Two Antimony (III) Oxalates as UV Optical Materials, *Inorg. Chem.*, 2023, **62**, 13148–13155.
- [26] Q. Wei, K. Wang, C. He, L. Wei, X. F. Li, S. Zhang, X. T. An, J. H. Li and G. M. Wang, Linear and Nonlinear Optical Properties of Centrosymmetric $\text{Sb}_4\text{O}_5\text{SO}_4$ and Noncentrosymmetric $\text{Sb}_4\text{O}_4(\text{SO}_4)(\text{OH})_2$ Induced by Lone Pair Stereoactivity, *Inorg. Chem.*, 2021, **60**, 11648–11654.
- [27] D. Zhang, Q. Wang, T. Zheng, L. Huang, L. L. Cao, D. J. Gao, J. Bi and G. H. Zou, $\text{NH}_4\text{Sb}_2(\text{C}_2\text{O}_4)\text{F}_5$: A Novel UV Nonlinear Optical Material Synthesized in Deep Eutectic Solvents, *J. Alloys Compd.*, 2022, **896**, 162921.
- [28] F. Yang, L. J. Huang, X. Y. Zhao, L. Huang, D. J. Gao, J. Bi, X. Wang and G. H. Zou, An Energy Band Engineering Design to Enlarge the Band Gap of KTiOPO_4 (KTP)-type Sulfates via Aliovalent Substitution, *J. Mater. Chem. C*, 2019, **7**, 8131–8138.
- [29] F. F. He, Y. W. Ge, X. Y. Zhao, J. He, L. Huang, D. J. Gao, J. Bi, X. Wang and G. H. Zou, Two-stage Evolution from Phosphate to Sulfate of New KTP-type Family Members as UV Nonlinear Optical Materials through Chemical Cosubstitution-oriented design, *Dalton Trans.*, 2020, **49**, 5276–5282.
- [30] Q. Wang, L. Wang, X. Y. Zhao, L. Huang, D. J. Gao, J. Bi, X. Wang and G. H. Zou, Centrosymmetric $\text{K}_2\text{SO}_4 \cdot (\text{SbF}_3)_2$ and Noncentrosymmetric $\text{Rb}_2\text{SO}_4 \cdot (\text{SbF}_3)_2$ Resulting from Cooperative Effects of Lone Pair and Cation Size, *Inorg. Chem. Front.*, 2019, **6**, 3125–3132.
- [31] Y. Lan, J. X. Ren, P. Zhang, X. H. Dong, L. Huang, L. L. Cao, D. J. Gao and G. H. Zou, $\text{ASb}(\text{SO}_4)_2$ ($\text{A} = \text{Rb}, \text{Cs}$): Two Short-wave UV Antimony Sulfates Exhibiting Large Birefringence

Chin. Chem. Lett., 2024, **35**, 108652.

- [32] C. H. Hu, X. T. Cai, M. F. Wu, Z. H. Yang, J. Han and S. L. Pan, Lone Pair-driven Enhancement of Birefringence in Polar Alkali Metal Antimony Phosphates, *Chem. Mater.*, 2022, **34**, 4224–4231.
- [33] F. F. He, L Wang, C. F. Hu, J. Zhou, Q. Li, L. Huang, D. J. Gao, J. Bi, X. Wang and G. H. Zou, Cation-tuned Synthesis of the $A_2SO_4 \cdot SbF_3$ ($A = Na^+, NH_4^+, K^+, Rb^+$) Family with Nonlinear Optical Properties, *Dalton Trans.*, 2018, **47**, 17486.
- [34] Y. Lan, H. Luo, L. L. Wang, L. Huang, L. L. Cao, X. H. Dong and G. H. Zou, Two Short-wave UV Antimony(III) Sulfates Exhibiting Large Birefringence, *Inorg. Chem.*, 2024, **63**, 2814–2820.
- [35] D. Zhang, Q. Wang, T. Zheng, L. Cao, K. M. Ok, D. Gao, J. Bi, L. Huang and G. H. Zou, Cation-anion Synergetic Interactions Achieving Tunable Birefringence in Quasi-one-dimensional Antimony(III) Fluoride Oxalates, *Sci. China Mater.*, 2022, **65**, 3115–3124.
- [36] F. Yang, L. Wang, Y. W. Ge, L. Huang, D. J. Gao, J. Bi and G. H. Zou, $K_4Sb(SO_4)_3Cl$: The First Apatite-type Sulfate Ultraviolet Nonlinear Optical Material with Sharply Enlarged Birefringence, *J. Alloys Compd.*, 2020, **834**, 155154.
- [37] V. Ya. Kavun, L. A. Zemnukhova and M. M. Polyantsev, Ion Mobility in Complex Antimony(III) Sulfate Fluorides $M_6Sb_4(SO_4)_3F_{12}$ ($M = Rb, Cs, NH_4$) and $(NH_4)_2Sb(SO_4)F_3$ According to ^{19}F and 1H NMR Data, *J. Struct. Chem.*, 2018, **59**, 47–52.